Original scientific paper

UDK 677.674:661.185
DOI 10.7251/COMEN2601072V

EFFECTS OF SOFT SEGMENT CONTENT AND LASER-INDUCED GRAPHENE ON THE SURFACE AND THERMAL PROPERTIES OF CROSS-LINKED POLYURTEHANES

Vanja Vojnović[1*], Marko Spasenović[1], Dana Vasiljević-Radović[1], Darko Micić[2], Marija V. Pergal[1]

[1] University of Belgrade, Institute of Chemistry, Technology and Metallurgy – National institute of the Republic of Serbia, Belgrade, Serbia
[2] University of Belgrade, Institute of General and Physical Chemistry, Belgrade, Serbia

[*] Corresponding author: vanja.vojnovic@ihtm.bg.ac.rs

Abstract: The versatile chemistry of polyurethanes (PUs) makes them suitable for a wide range of applications. In particular, surface topography and thermal behavior can be effectively tailored by adjusting the soft segment content (SSC) within the PU structure. However, as an intrinsically nonconductive class of polymers, PUs are not suitable for electronic applications. With the increasing interest in polymer/graphene heterostructures, the formation of graphene conductive pathways on polymer surfaces has emerged as a promising approach to overcome this limitation. In this study, we systematically examined the effects of varying SSC (expressed in wt.%) in synthesized cross-linked PUs, as well as the influence of laser-induced graphene (LIG) transferred onto the PU surface on several key properties: surface roughness *via* atomic force microscopy (AFM), surface wettability using water contact angle (WCA) measurements, and thermal properties through differential scanning calorimetry (DSC). An increase in SSC led to a reduction in surface roughness and a concomitant increase in WCA, indicating enhanced hydrophobicity. The presence of LIG further augmented the hydrophobic character of the surface. The PU structure exhibited a pronounced effect on both glass transition (T_g) and melting temperatures (T_m), while LIG had a minimal impact on thermal properties. This research provides a framework for engineering the surface and thermal properties of PU-based materials for applications in flexible electronics and smart coatings.

Keywords: polymers, composites, structure-property relationship, AFM, WCA, DSC.

1. INTRODUCTION

Polyurethanes (PUs) represent a broad and versatile class of polymers that include thermoplastics, thermosets, flexible and rigid foams, adhesives, and waterborne formulations. They exhibit a wide range of structures, properties, and applications, with their primary structural commonality being the urethane linkage (–NH–CO–O–), typically formed through reactions between isocyanates and polyols [1,2].

Thermoset or chemically cross-linked PUs based on poly(dimethylsiloxane) (PDMS) are particularly attractive due to their improved elasticity, biocompatibility [3,4], corrosion and thermal resistance [5], and enhanced hydrophobicity [4]. Tailoring surface roughness and wettability underscores the strong structure–property relationship in PUs. Surface and thermal characteristics of PUs are of special importance for purposes such as self-cleaning, protective clothing, stimuli-responsive smart coatings, marine antifouling, and anticorrosion coatings [6].

For the fabrication of durable, flexible electronic devices with desired characteristics, polymer/graphene heterostructures have emerged as a promising solution [3,7]. Laser-induced graphene (LIG) has

recently gained attention as an innovative and scalable method for producing conductive patterns by laser irradiation of a suitable substrate surface (e.g., commercial polyimide, PI) [8].

However, for the polymers that lack in aromatic structures, like aliphatic PUs [9], silicone-based substrates [10] or poly(methylmethacrylate) (PMMA) [11], direct laser induction graphene is not feasible. In these cases, transfer approaches have been developed to improve adhesion and wettability of LIG films [12]. The morphology [13] and wettability [14] of LIG can be readily adjusted by many methods, including altering lasering parameters, changing induction atmosphere [16,17], or through in situ fluorination [15,17].

This work is a continuation of research on LIG/PU materials [3], with emphasis on surface and thermal properties to expand the potential applications. In this study, we systematically investigated the effects of varying soft segment content on surface roughness by atomic force microscopy (AFM), wettability by static water contact angle measurements and thermal behavior by differential scanning calorimetry (DSC). This study provides further insight into designing PU-based materials for advanced applications in coatings and flexible electronics.

2. MATERIALS AND METHODS

2.1. Material Synthesis

Laser-induced graphene (LIG) was produced on commercial polyimide substrate according to the procedure described by Vićentić et. al. [7], and subsequently transferred onto the synthesized PUs. Thermoset polyurethane was synthesized *via* two-step polyaddition reaction in a solution. For the synthesis, we used α,ω-dihydroxyethoxy poly(dimehylsiloxane) (EO-PDMS) pretpolymer as a part of the soft segments (SS), while 4,4′-methylenediphenyl diisocyanate (MDI) and hyperbranched polyester of the second pseudo generation (BH-20) crosslinker as a part of hard segments (HS), $Sn(Oct)_2$ catalyst and a THF/NMP solvent mixture. The SS:HS ratios were adjusted to 30:70, 40:60, and 50:50, denoted as PU-30, PU-40, and PU-50, respectively. All materials investigated in this study were synthesized and structurally characterized in our previous work reported by Vojnović et. al. [3].

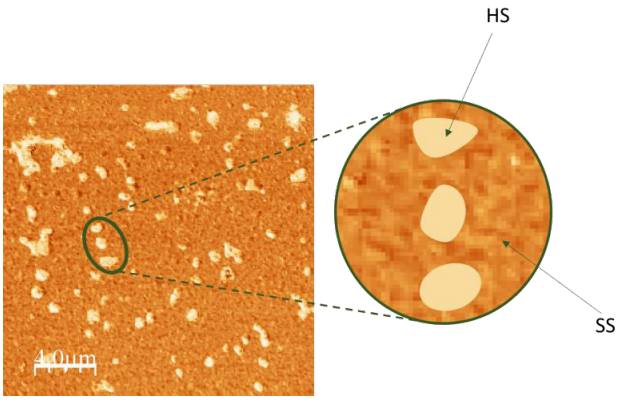

Figure 1. *Schematic representation of cross-linked polyurethanes: SS – soft segments (darker regions), HS – hard segments (brighter regions).*

2.2. Characterization Methods

Static water contact angle (WCA) measurements were performed at room temperature using a goniometer (Ossila, The Netherlands) with distilled water. Thin PU and LIG/PU films were placed on a flat holder with double-sided adhesive tape to ensure flat surface for the reliable experiment. Results are given as an average value obtained from five different surface droplet positions with its standard deviations (WCA±SD).

Surface topography data (root mean square roughness, arithmetic average roughness, average height, and peak-to-peak values) of the synthesized PUs were obtained by atomic force microscopy (NTEGRA Prima atomic force microscope, NT-MDT) in the intermittent-contact mode at a scan size of 30×30 μm^2. WSxM 4.0 software (v. beta 9.3) [18] was used to analyze images. WCA and AFM experiments were conducted under ambient conditions.

Thermal transitions were analyzed *via* differential scanning calorimetry (DSC, Q1000, TA Instruments, USA). All DSC scans were conducted in the temperature range from – 90 to 260 °C, in three cycles: the first heating cycle from – 90 to 260 °C, the second cooling cycle from 260 to – 90 °C and the third heating cycle from – 90 to 260 °C, at heating and cooling rates of 10 and 5 °C min^{-1}, respectively. The samples (each weighted ~ 7 mg) were placed in aluminum pans. TA Advantage/Universal Analysis 2000 software (v. 4.5 A) was used for thermogram analysis.

3. RESULTS AND DISCUSSION

Polyurethanes with varying soft segment content in their structure, along with the subsequent transfer of laser-induced graphene onto PU thin films, were thoroughly characterized in the work of Vojnović et al. [3]. These materials previously demonstrated stability as pulse rate sensors in humid environments, but for further application in coatings and flexible electronics, it is essential to understand how their surface characteristics and thermal transitions are governed by composition and LIG quality.

3.1. Atomic Force Microscopy

Intermolecular hydrogen bonding between NH and C=O groups within the urethane hard segments plays a key role in phase separation and the development of surface topography in PDMS-based PUs [18]. Atomic force microscopy was employed to examine the surface topography of PUs and to establish a correlation with HS/SS ratio in the polymer structure, which later impact surface wettability and thermal transitions in the samples. PU-30 exhibits the highest RMS roughness (Table 1), with pronounced bright domains corresponding to aggregated hard segments organized in partially ordered clusters (Figure 1). This indicates limited compatibility between PDMS soft domains and the urethane-based hard domains at lower SSC, leading to microphase separation and heterogeneous surface relief.

As SSC increases, both RMS roughness and peak-to-peak values decrease, with PU-50 showing the smoothest and most homogeneous morphology. The average height parameter also follows this trend, confirming that higher PDMS content leads to a more uniform distribution of domains and suppression of large hard-segment aggregates. The reduced roughness in PU-50 correlates with enhanced microphase mixing and improved flexibility, consistent with earlier mechanical tests [3]. Concrete values of these parameters are listed below (Table 1).

These observations highlight that the interplay between hydrogen bonding density and PDMS content critically dictates surface topography. Smooth and homogeneous surfaces (PU-50) are beneficial for electronic device integration, since they minimize defect formation at the PU/LIG interface.

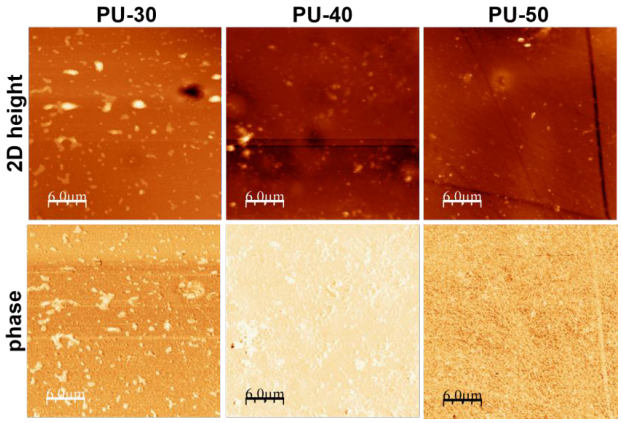

Figure 2. *2D height and phase AFM images of the prepared PU materials.*

Table 1. *Data extracted from AFM analysis.*

Material	R_q (nm)*	R_a (nm)**	Average height (nm)	Peak to peak (nm)	Water contact angle (°)
PU-30	49.3	29.3	277.3	747.8	78±3
PU-40	29.3	19.0	89.8	532.6	86±3
PU-50	20.2	13.8	82.4	402.1	91±1

*root mean square roughness and **arithmetic average roughness

3.2. Water Contact Angle Measurements

Control of wettability of materials is crucial for applications in self-cleaning surfaces, antifouling coatings, and biomedical devices [6]. The composition of polyurethanes, specifically the content of soft segments [4] or hard segments [19], significantly influences the wetting characteristics of these polymers. It is well-established that PDMS has low surface energy exhibiting a WCA exceeding 100° [20]. According to this deliberation, PUs with a higher wt. % of PDMS macrodiol in their structure are likely to exhibit enhanced hydrophobicity. This assumption is supported by results from static water contact angle measurements, where WCA increases in the following order: PU-30 < PU-40 < PU-50, hence altering the surface wettability from hydrophilic (WCA < 90°) to hydrophobic (WCA > 90°). Figure 3, b). Namely, PU-30 exhibits WCA < 90°, placing it in the hydrophilic regime, while PU-40 and PU-50 progressively increase WCA, with PU-50 crossing into

the hydrophobic domain (Table 1, Figure 3b). This progression from hydrophilic to hydrophobic with higher SSC directly reflects the dominant contribution of PDMS to the surface chemistry.

In the same manner, WCAs were assessed for LIG transferred onto PUs with varying SSC *via* spin coating. A commercially available polyimide sheet served as a hydrophilic parent substrate (refer to the dashed line in Figure 3, a)) for the LIG transfer. While LIG produced on PI showed superhydrophilic nature as a result of partial oxidation occurring in the air [8,14], the transfer process flips the oxygen-rich LIG side, resulting in WCAs values of approximately 140° (Figure 3), which gives bordering superhydrophobic surfaces. All LIG materials exhibit comparable WCA values (WCA = 138° for LIG/PU-30; WCA = 140° for LIG/PU-40, and WCA = 143° for LIG/PU-50), which is anticipated due to the same parent substrate utilized in LIG production. Such high WCAs approach the superhydrophobic threshold, indicating that the LIG transfer process creates surfaces highly resistant to water wetting. Interestingly, all LIG/PU composites show nearly identical WCA values regardless of SSC, since the LIG layer dominates surface properties. This can be the main reason for minimal cross-sensitivity to humidity [3]. This finding is particularly relevant for sensor applications in humid conditions. Luong et al. [12] observed a similar behavior for transferred LIG, while Li et al. [15] produced hydrophobic films through vacuum filtration using LIG powder scratched off the substrate. The present results confirm that transferred LIG provides a robust, composition-independent hydrophobic coating.

3.3. Differential Scanning Calorimetry

Semi-crystalline PUs contain randomly distributed hard segments within the PDMS matrix and therefore possess both glass transitions (associated with amorphous regions) and melting transitions (associated with crystalline regions). Differential scanning calorimetry shows these transitions during the first heating scan for all the investigated materials

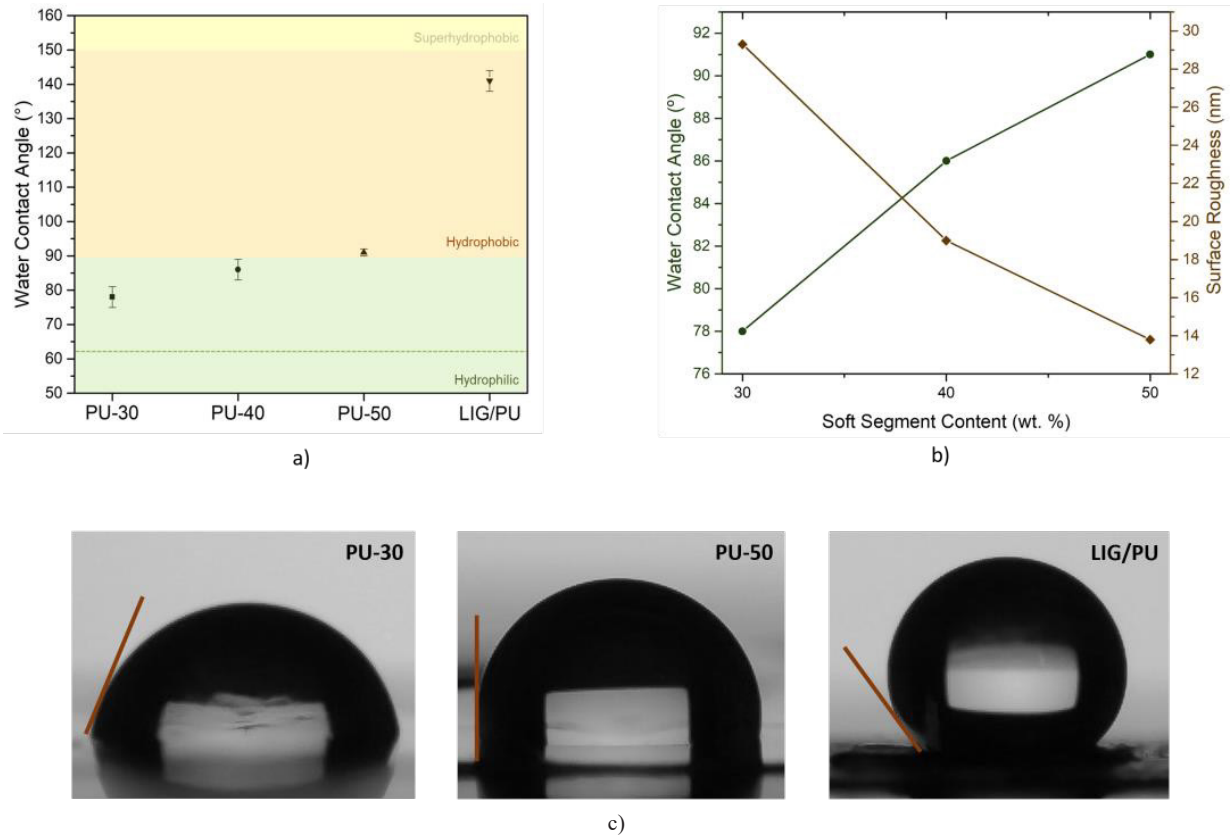

Figure 3. *a) Static water contact angles of pure PUs and average WCA of LIG/PUs; b) Water contact angles and surface roughness with varying SSC in PU matrix; and c) From hydrophilic to bordering superhydrophobic surfaces.*

(see Figure 4 and Table 2). While soft segments affect the thermal stability of polyurethanes [21], a hydrogen bonds in hard segments exert a greater influence on the thermal properties [22]. Hard segments exhibit a high glass transition temperature, whereas PDMS is recognized for its exceptionally low T_g of around – 123 °C [5,23] but this low T_g is out of scope of our instrument (– 90 °C to 260 °C).

DSC analysis of the first heating scans (Figure 4, Table 2) reveals that T_g decreases systematically with increasing SSC: PU-30 shows the highest T_g, while PU-50 exhibits the lowest. This trend reflects the plasticizing effect of PDMS, which lowers the segmental mobility threshold temperature [24]. The observed reduction in T_g aligns with mechanical results where PU-50 displayed the greatest flexibility [3]. It is anticipated that this category of PUs will exhibit a moderate to high T_g. Values for T_g obtained from DSC experiment suggest that expected trend was observed, and PU-50 with a balanced ratio of SS/HS exhibited the lowest glass transition temperature in the series (Table 2).

The melting temperatures (T_m) associated with hard-segment crystalline domains show a slight decrease with higher SSC. This can be attributed to reduced packing efficiency of hard segments when diluted by flexible PDMS chains. Moreover, stronger hydrogen bonding within densely packed hard domains in PU-30 stabilizes crystalline order, whereas in PU-50, lower HS density leads to smaller and less ordered crystallites, lowering T_m [25,26].

Comparison of the first (C_1) and second (C_3) heating scans (Table 2) confirms the elimination of thermal history in C_3, which results in slightly lower and more reproducible glass transition temperatures. For PU-30 samples, T_g decreases from 55.8 °C to 48.9 °C (PU-30_{st}) and from 47.1 °C to 47.7 °C (PU-30_{sc}), while the melting temperatures increase, indicating that initial crystalline domains reorganize into more stable structures after the first heating. In contrast, PU-40 and PU-50 exhibit a decrease in T_g (from 50.8 °C to 46.6 °C and from 43.8 °C to 41.7 °C, respectively), but no detectable T_m in C_3. This absence of melting peaks demonstrates that crystal-

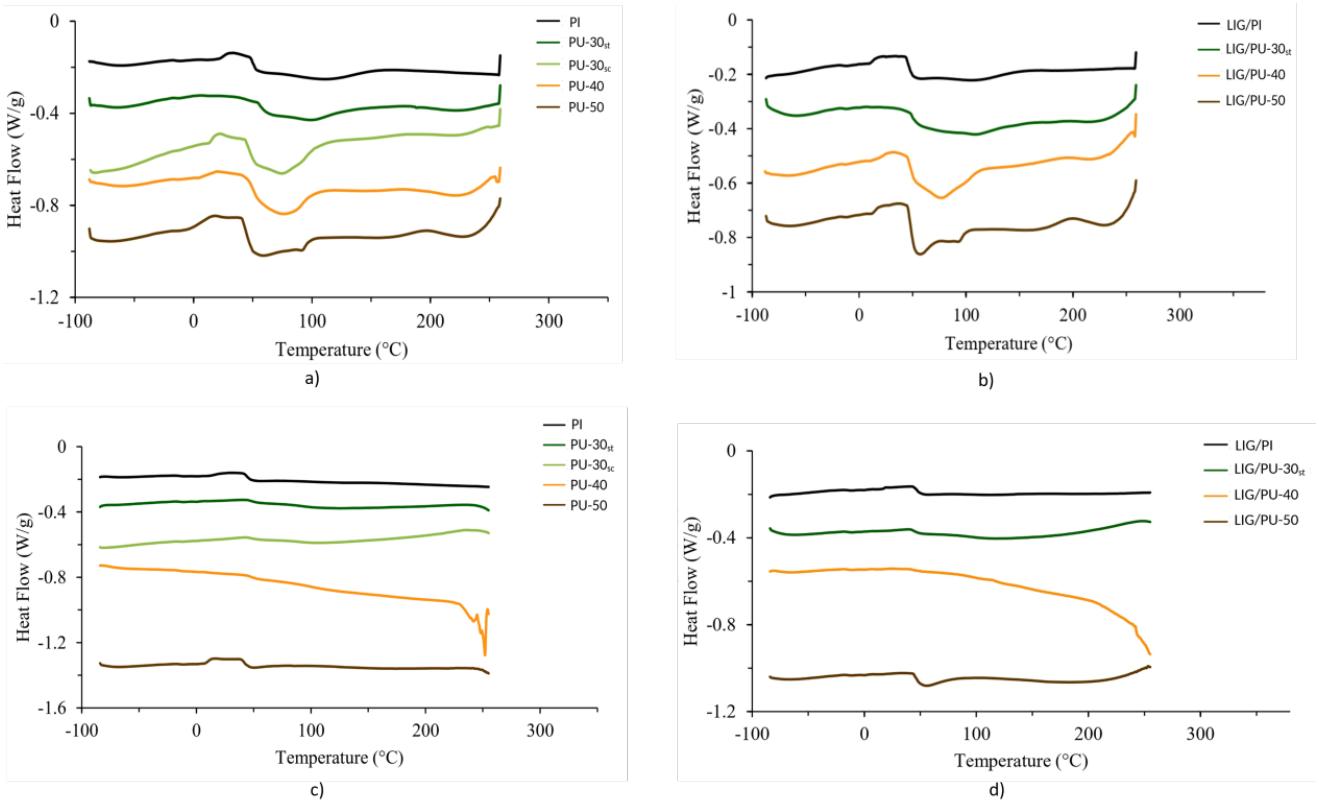

Figure 4. *DSC thermograms: a), b) for the C1 scan, and c), d) for the C3 scan. Samples are denoted in the figure. The samples are marked in the figure.*

line hard-segment domains, once disrupted in the first cycle, cannot recrystallize during cooling due to the dominant amorphous character and the higher PDMS content. These findings underline the metastable nature of hard-segment crystallinity in PDMS-based PUs with higher SSC.

A greater degree of branching or cross-linking in the polymer, and a higher density of hydrogen bonds within the hard domains can results in reduced melting temperatures in comparison to linear polyurethanes [25,26]. Obtained results of DSC analysis in corresponding LIG/PU materials showed negligible changes in thermal behaviors. Similar result was previously observed [27]. In the conclusion, thermal behavior of polyurethanes and its composites is mostly governed by the soft and hard segments ratios, and thin LIG film on the surface has minimal impact on thermal stability of the composites.

Table 2. Results of DSC analysis.

	C_1		C_3	
Material	T_g (°C)	T_m (°C)	T_g (°C)	T_m (°C)
PI	49.7	113.3	44.1	-
PU-30$_{st}$	55.8	100.4	48.9	112.3
PU-30$_{sc}$	47.1	77.0	47.7	105.0
PU-40	50.8	78.8	46.6	-
PU-50	43.8	91.8	41.7	-
LIG/PI	47.1	112.2	47.5	-
LIG/PU-30$_{st}$	49.6	110.4	44.4	117.7
LIG/PU-40	47.9	78.1	42.6	-
LIG/PU-50	46.6	93.4	44.8	-

4. CONCLUSION

In this study, cross-linked polyurethanes with different soft segment contents (30, 40, and 50 wt.% SSC) and their LIG/PU counterparts were systematically characterized using AFM, WCA, and DSC techniques. The results demonstrate that hydrogen bonding within hard segments significantly influences the surface topography of PDMS-based PUs. Increasing SSC leads to smoother and more homogeneous surfaces, consistent with enhanced microphase mixing.

Wettability analysis revealed that SSC is the dominant factor controlling surface hydrophobicity. PU-30 exhibited hydrophilic behavior, while PU-50 became distinctly hydrophobic, reflecting the low surface energy of PDMS. After LIG transfer, all PU surfaces achieved water contact angles above 140°, approaching superhydrophobicity, irrespective of SSC. This finding indicates that LIG layers provide a robust strategy for humidity resistance and moisture stability, which is crucial for sensor and coating applications.

DSC analysis showed that thermal transitions are primarily determined by the relative balance of soft and hard segments. Increasing SSC lowered the glass transition temperature due to the plasticizing effect of PDMS, while melting transitions associated with hard domains shifted slightly to lower values as the HS fraction decreased. Importantly, the presence of a thin LIG layer had negligible influence on bulk thermal properties, confirming that its effect is limited to surface modification.

Overall, this work establishes that tailoring the PU composition combined with LIG transfer enables simultaneous optimization of surface hydrophobicity and thermal behavior. These insights provide a foundation for designing LIG/PU-based materials with high potential in durable, flexible electronics operating under humid conditions, as well as in advanced smart coatings, including self-cleaning, anticorrosion, and antifouling applications.

ACKNOWLEDGEMENTS: This research was supported by the Science Fund of the Republic of Serbia, #4950, Polymer/graphene heterostructures for physiological sensors — Polygraph. The authors also would like to thank the Ministry of Science, Technological Development, and Innovation of the Republic of Serbia (Contract No: 451-03-136/2025-03/200026).

5. REFERENCES

[1] J. O. Akindoyo, et al., *Polyurethane types, synthesis and applications – a review*, RSC Advances, Vol. 6−115 (2016) 114453–114482.
[2] F. M. De Souza, et. al., *Materials and Chemistry of Polyurethanes*, American Chemical Society, Washington DC 2021, 1–36.
[3] V. Vojnović, et al., *Pulse Sensors Based on Laser-Induced Graphene Transferred to Biocompatible Polyurethane Networks: Fabrication,*

Transfer Methods, Characterization, and Application, Chemosensors, Vol. 13–4 (2025) 122.

[4] M. V. Pergal, et al., *Structure and properties of thermoplastic polyurethanes based on poly(dimethylsiloxane): Assessment of biocompatibility: Structure, Properties and Biocompatibility of TPUs*, Journal of Biomedical Materials Research Part A, Vol. 102–11 (2014) 3951–3964.

[5] M. Taşdemir, et al., *Investigation of corrosion and thermal behavior of PU–PDMS-coated AISI 316L*, e-Polymers, Vol. 21−1 (2021) 355–365.

[6] W. Tian, et al., *Polyurethane coatings modified by OH-PDMS for anti-cavitation, antifouling and anticorrosion applications*, Progress in Organic Coatings, Vol. 179 (2023) 107515.

[7] T. Vićentić, et al., *Laser-Induced Graphene for Heartbeat Monitoring with HeartPy Analysis*, Sensors, Vol. 22−17 (2022) 6326.

[8] J. Lin, et al., *Laser-induced porous graphene films from commercial polymers*, Nature Communications, Vol. 5−1 (2014) 5714.

[9] Matějka, et. al., *Structure evolution during order–disorder transitions in aliphatic polycarbonate based polyurethanes. Self-healing polymer*, Chemical Engineering Journal, Vol. 357 (2019) 611−624.

[10 Jiuqiang Li, et al., *Laser-Induced Graphene-Assisted Patterning and Transfer of Silver Nanowires for Ultra-Conformal Breathable Epidermal Electrodes in Long-Term Electrophysiological Monitoring*, Adanced Functional Materials, Vol. 35 (2025) 2504481.

[11 G. Antonelli, et al., *Laser-induced graphene wet transfer technique for lab-on-chip applications*, Sensors and Actuators A: Physical, Vol. 377 (2024) 115746.

[12 D. X. Luong, et al., *Laser-Induced Graphene Composites as Multifunctional Surfaces*, ACS Nano, Vol. 13−2 (2019) 2579–2586

[13 S. Hong, et al., *Surface Morphological Growth Characteristics of Laser-Induced Graphene with UV Pulsed Laser and Sensor Applications*, ACS Materials Letters, Vol. 5−4 (2023) 1261–1270.

[14 J. Nasser, et al., *Laser induced graphene printing of spatially controlled super-hydrophobic/hydrophilic surfaces*, Carbon, Vol. 162 (2020) 570–578.

[15 Y. Li, et al., *Laser-Induced Graphene in Controlled Atmospheres: From Superhydrophilic to Superhydrophobic Surfaces*, Advanced Materials, Vol. 29–27 (2017) 1700496.

[16 A. Dallinger, et al., *Different Roles of Surface Chemistry and Roughness of Laser-Induced Graphene: Implications for Tunable Wettability*, ACS Applied Nano Materials, Vol. 6–18 (2023) 16201–16211.

[17 K.-H. Nam, et al., *Laser-Induced fluorinated graphene for superhydrophobic surfaces with anisotropic wetting and switchable adhesion*, Applied Surface Science, Vol. 574 (2022) 151339.

[18 I. Horcas, et al., *WSXM: a software for scanning probe microscopy and a tool for nanotechnology*, Review of Scientific Instruments, Vol. 78–1 (2007) 013705.

[19 Yilgör E and Yilgör İ., *Influence of soft segment structure, hydrogen bonding, and diisocyanate symmetry on morphology and properties of segmented thermoplastic polyurethanes and polyureas*. Turkish Journal of Chemistry, Vol. 47-5 (2023) 1007-1017.

[20 B. Ruben, et al., *Oxygen plasma treatments of polydimethylsiloxane surfaces: effect of the atomic oxygen on capillary flow in the microchannels*, Nano-Micro Letters, Vol. 12–10 (2017) 754–757.

[21 L. Shufen, et al., *Studies on the Thermal Behavior of Polyurethanes*, Polymer-Plastics Technology and Engineering, Vol. 45–1 (2006) 95–108.

[22 Amado, J.C.Q., *Thermal Resistance Properties of Polyurethanes and Its Composites*, IntechOpen, Rijeka 2019, Chapter 5, 1–13.

[23 M. V. Pergal, et al., *Poly(urethane–siloxane) s based on hyperbranched polyester as cross-linking agent: synthesis and characterization*, Journal of Serbian Chemical Society. Vol. 77–7 (2012) 919–935.

[24 F. De Rossi, et al., *Thermosetting polyurethane-based encapsulation of flexible perovskite solar cells: A step forward in devices stabilization in highly damp environment*, Materials Today Energy, Vol. 49 (2025) 101850.

[25 Somdee, et. al., *Thermal analysis of polyurethane elastomers matrix with different chain extender contents for thermal conductive appli-*

cation, Journal of Thermal Analysis and Calorimetry, Vol. 138, 1003–1010 (2019).

[26] J. Brzeska, et. al., *Branched Polyurethanes Based on Synthetic Polyhydroxybutyrate with Tunable Structure and Properties*, Polymers, Vol. 10–8 (2018) 826.

[27] M. V. Pergal, et al., *Laser-Induced Graphene on Novel Crosslinked Poly(dimethylsiloxane)/Triton X-100 Composites for Improving Mechanical, Electrical and Hydrophobic Properties*, Polymers, Vol. 16–22 (2024) 3157.

УТИЦАЈ САДРЖАЈА МЕКИХ СЕГМЕНАТА И ЛАСЕРСКИ-ИНДУКОВАНОГ ГРАФЕНА НА ПОВРШИНСКА И ТЕРМИЧКА СВОЈСТВА УМРЕЖЕНИХ ПОЛИУРЕТАНА

Сажетак: Разноврсна хемија полиуретана (ПУ) чини ове полимере погодним за најразличитије примене. Површинска топографија и термичка својства се на једноставан начин могу подешавати варирањем меких сегмената (SSC) на бази поли(диметилсилоксана) (ПДМС) у ПУ матрици. Због недостатка електричне проводности, ПУ полимери, нису погодни за примену у електроници. Међутим, са порастом интересовања за полимер/графен хетероструктуре, креирање графенских проводних структура на површини полимера се показало као добро решење за вишенаменске савитљиве електронске уређаје. У овом истраживању систематски је испитан утицај различитих масених процената SSC на синтетисане умрежене ПУ, као и утицај пренетог ласерски-индукованог графена (ЛИГ) на ПУ филмове, и то на храпавост површине помоћу микроскопије атомских сила (AFM), квашљивост површине мерењем углова квашења (WCA), као и на термичка својства користећи диференцијалну скенирајућу калориметрију (DSC). Са порастом SSC смањује се храпавост површине, док истовремено долази до повећања WCA, а ЛИГ додатно утиче на пораст хидрофобности површине. Састав ПУ значајно утиче на температуре остакљивања и топљења, док сам ЛИГ има минималан утицај на термичка својства материјала. Ово истраживање нуди стратегије за подешавање површинских и термичких својстава материјала на бази ПУ за примену у флексибилној електроници и паметним превлакама.

Кључне речи: полимери, композити, однос структура–својства, AFM, WCA, DSC.

Paper received: 25 August 2025 **Paper accepted: 7 April 2026**